AGU ADVANCING EARTH AND SPACE SCIENCE

Water Resources Research®

RESEARCH ARTICLE
10.1029/2020WR029124

On the Impact of Rainfall Spatial Variability, Geomorphology, and Climatology on Flash Floods

Manabendra Saharia[1,2,3,4], Pierre-Emmanuel Kirstetter[1,2,5,6], Humberto Vergara[3], Jonathan J. Gourley[6], Isabelle Emmanuel[7], and Hervé Andrieu[7]

[1]School of Civil Engineering and Environmental Science, University of Oklahoma, Norman, OK, USA, [2]Advanced Radar Research Center, University of Oklahoma, Norman, OK, USA, [3]Cooperative Institute for Mesoscale Meteorological Studies, Norman, OK, USA, [4]Now at Department of Civil Engineering, Indian Institute of Technology Delhi, New Delhi, India, [5]School of Meteorology, University of Oklahoma, Norman, OK, USA, [6]NOAA/National Severe Storms Laboratory, Norman, OK, USA, [7]GERS-LEE, University of Gustave Eiffel, IFSTTAR, Bouguenais, France

Key Points:

- The impact of rainfall spatial variability, physiography and climatology on flood severity is empirically investigated for the first time
- Severity increases with basin slope and accumulated precipitation, and decreases with rainfall dispersion w.r.t. the flow path
- Basin physiography dampens the effect of lower rainfall intensities, while higher rainfall overwhelms other factors

Correspondence to:
P.-E. Kirstetter,
pierre.kirstetter@noaa.gov

Citation:
Saharia, M., Kirstetter, P.-E., Vergara, H., Gourley, J. J., Emmanuel, I., & Andrieu, H. (2021). On the impact of rainfall spatial variability, geomorphology, and climatology on flash floods. *Water Resources Research*, *57*, e2020WR029124. https://doi.org/10.1029/2020WR029124

Received 28 OCT 2020
Accepted 19 AUG 2021

Abstract The effects of spatial variability of rainfall, geomorphology, and climatology of precipitation and temperature on the hydrologic response remain poorly understood. This study characterizes the catchment response in terms of a variable called flashiness, that describes the severity of the flood response as the rate of rise of the unit discharge. It overcomes limitations of prior works based on limited case studies or simulations by gathering information on basins of widely varying characteristics and by using a high-resolution rainfall and flooding event data set spanning 10 years over the Continental United States. The objective is to develop a robust understanding of how rainfall spatial variability influences flash flood severity and to assess its contribution relative to basin physiography and climatology. This study explores the first-order dependencies as well as the variability in these relationships and investigates the complex interactions using a multi-dimensional statistical modeling approach. The results confirm that the spatial organization of rainfall influences the basin response on par with geomorphology and climatology. Basin physiography dampens the effect of lower rainfall intensities, while higher rainfall overwhelms other factors and primarily contributes to flashiness. Dispersion of precipitation with respect to the flow path decreases flood severity. An improved understanding of sub-basin scale rainfall spatial variability aids in developing a robust flash flood severity index to identify and mitigate flash flooding situations as well as identifying basins which could most benefit from distributed hydrologic modeling.

Plain Language Summary This study aims at understanding the effects of rainfall, geomorphology, and climatology on the flash flood response at the hydrologic event scale. To investigates, these interactive processes, it uniquely gathers information on basins of widely varying characteristics and by using a high-resolution rainfall and flooding event data set spanning 10 years over the Continental United States. The results confirm that the spatial organization of rainfall influences the basin response on par with geomorphology and climatology. Basin physiography dampens the effect of lower rainfall intensities, while higher rainfall overwhelms other factors and primarily contributes to the flood response. Dispersion of precipitation with respect to the stream network decreases flood severity. An improved understanding of the rainfall spatial variability at sub-basin scale aids in identifying and mitigating flash flooding situations.

1. Introduction

Rainfall is a highly heterogeneous process over a wide range of scales in space and time (Fabry, 1996; Marani, 2005; Rodriguez- Iturbe & Rinaldo, 1997) and the influence of rainfall spatial variability on hydrologic response of watersheds has been a recurrent theme in hydrology for decades. The increasing usage of distributed hydrologic models and availability of high-resolution rainfall data in recent decades has resulted in an increasing number of studies in this area.

The extent to which spatial heterogeneity of rainfall impacts catchment response and its influence in comparison to basin physiography and climatology remains an open research topic. The literature has not yielded a consensus, which has implications for understanding flood processes and adequately representing them in distributed hydrologic models for improved forecasting of floods. While studies typically based on

hydrological modeling results have concluded that the spatial variability of rainfall exerts a significant impact on the hydrograph (Anquetin et al., 2010; Kim et al., 2008; Looper & Vieux, 2012; Mei et al., 2014; Sangati et al., 2009; Smith et al., 2007; Vieux et al., 2009; Zoccatelli et al., 2010), others have indicated limited influence of rainfall spatial variability (Adams et al., 2012; Brath et al., 2004; Cole & Moore, 2008; Nicótina et al., 2008; Smith et al., 2004). Pokhrel and Gupta (2011) have reported that the influence of rainfall spatial variability on the hydrologic response can be greatly diminished by the dampening effect of routing, while Lobligeois et al. (2014) concluded that there is a regional dependence.

By mostly using distributed hydrologic models, past studies may have unduly stressed model sensitivity instead of observed sensitivity (Marra & Morin, 2015; Obled et al., 1994; Smith et al., 2004; Winchell et al., 1998). Smith et al. (2004) expressed reservations about using distributed hydrologic models to study the importance of rainfall spatial variability, which may introduce more uncertainty in the results due to errors in data, model structure, and parameters. Moreover, most of these contributions are performed on a case study basis covering a few events, which limits our ability to make generalizations applicable to a wide variety of scenarios. A few studies have attempted to address this shortcoming. For example, Emmanuel et al. (2015) adopted a simulation chain that combines a stream network model, a rainfall simulator, and a distributed hydrologic model to disentangle the relationship between rainfall spatial variability and runoff. This study tested the spatial rainfall variability indices described in Zoccatelli et al. (2010) and proposed two new indices that summarize the spatial organization of rainfall. By synthetically generating 9,900 simulated hydrologic events for hundreds of varying catchment sizes and rainfall types, they found that the organization of rainfall has an important influence on the catchment response.

A literature review reveals that our understanding of the impact of rainfall spatial variability on flooding under a wide variety of rainfall, physiographic, and antecedent conditions remain limited. It is important to develop frameworks to systematically analyze a variety of space-time scales and a variety of basin physiographic characteristics to capture diverse processes. At larger spatial scales, catchment responses are often simpler as much of the hydrologic system heterogeneity is subsumed and averaged (Sivapalan et al., 2003). At smaller spatial scales, hydrologic processes such as runoff are more intricately linked to details of landscape structure, thereby exhibiting greater space-time variability (Merz & Blöschl, 2004). The spatial variability in precipitation also adds to the variability in response by partially activating sub-basins to produce hydrologic responses that may vary depending on the intensity of rainfall; these sub-basin processes are prevalent when the storm size is smaller than the area of the entire catchment. To analyze the role of spatial rainfall variability in the analysis of flood generation, Woods and Sivapalan (1999) proposed an analytical method to express the variability of catchment-averaged storm runoff rates in terms of space and time variability of hydrological inputs. Smith et al. (2002, 2005) considered the rainfall-weighted centroid distance to the basin outlet that varies with time, whose mean value characterizes the rainfall pattern at the event scale. They represent the spatial variability of rainfall excess at the scale of a rain event by introducing the average rainfall excess with flow distance. Zoccatelli et al. (2011) proposed a set of spatial rainfall statistics known as "spatial moments of catchment rainfall" to assess the dependence of the catchment flood response on the space-time interaction between rainfall and the spatial organization of catchment flow pathways.

Large observational data sets have the potential to add much needed information beyond what is provided in the literature, the latter of which is typically based on distributed hydrological models that often introduce additional uncertainties beyond the observational data. This study seeks to fill an important gap by proposing to analyze the impact of rainfall spatial variability on basin response using a database of observed flood events. Quality-controlled radar rainfall data of high spatial and temporal resolution are used to compute the rainfall variability indices described in Zoccatelli et al. (2011) and Emmanuel et al. (2015). They are further combined with a large number of geomorphological and climatological attributes to develop a unique observational database suitable for clarifying the dependence between rainfall spatial organization, basin morphology, and catchment response. As severe floods cause great damage to life and property, we seek to investigate the flood response in term of flashiness, a hitherto unexplored aspect of the hydrograph in the context of rainfall spatial variability. Flashiness is introduced in Saharia et al. (2017) to represent the severity of floods. It gives the rate of rise of the hydrograph during flooding conditions and thus captures both the magnitude and timing aspects with higher values corresponding to more severe floods (Equation 2 in Saharia et al., 2017). Especially, it identifies basin responses with a high-magnitude discharge in a short

period of time. Flashiness provides a process-based interpretation of flash flood severity that differs from classical frequentist approaches based on peak discharge.

To the best of our knowledge, this study explores for the first time not only first-order dependencies of flashiness on event-level rainfall spatial variability, but also the variability in among these relationships using a big data approach. The relative impact of various rainfall and physiographic properties on flooding are quantified using a multi-dimensional modeling framework and the impact of the individual attributes are disaggregated. The purposes of this study are to (a) characterize flash flood severity (as represented by flashiness) using rainfall spatial variability and geomorphological parameters, (b) investigate the complexity of the underlying processes through the variation in these relationships, (c) quantify the relationship between rainfall spatial variability and flood response, and its contribution to flooding relative to basin morphology, and (d) identify which variables are most important to explain flashiness. In particular, Smith et al. (2004) considered it important to not just determine where great spatial variability of rainfall exists, but also to identify circumstances where the variability of rainfall overcomes the filtering effects of a physical basin to significantly impact the hydrologic response. Overall, the determination of the most relevant rainfall spatial organization factors for flash floods can be identified as an important exercise that will provide diagnostic capability to identify basins in which distributed hydrologic modeling is expected to be most effective.

The study is organized as follows. Section 2 describes the flood, physiographic, and rainfall data sets, and an overview of how the archive was developed. Section 3 describes the rainfall spatial variability indices and Section 4 presents a case study explaining these indices for a flooding event. Sections 5 and 6 characterize flash flood severity based on rainfall spatial variability indices and a large number of physiographic variables. Finally, Section 7 provides a summary of findings and concluding remarks.

2. Data Sets

2.1. The Unified Flash Flood Database

The flooding data is derived from the publicly available Unified Flash Flood Database described in Gourley et al. (2013), a unique data set subjected to extensive post-processing to harmonize data from a variety of sources over a long period. The database has been created by curating flooding information such as gauge streamflow measurements by US Geological Survey (USGS), flash flooding reports in the National Weather Service Storm Events Database, and public survey responses on flash flood impacts collected during the Severe Hazards Analysis and Verification Experiment (Gourley et al., 2010; Ortega et al., 2009). Flooding thresholds for USGS stream gauge locations defined by the NWS, in collaboration with local stakeholders, are used to extract flooding events from the streamflow record. The valuable information collected directly from the public during SHAVE, geographical coverage of NWS reports, and the automated streamflow measurement records of USGS makes it one of the most spatially and temporally representative flash flood databases at continental scale. It is publicly available for no cost at: https://blog.nssl.noaa.gov/flash/database/.

The times series information from the USGS component of the database is suitable for analyzing the impact of rainfall spatial variability on floods because it contains most of the necessary attributes such as flooding rise time, peak discharge, basin area, etc. This study utilizes the automated instantaneous streamflow measurements that the USGS collects at intervals ranging from 5 to 60 min for more than 10,000 gauges across the U.S. Correspondingly, the NWS has defined stages corresponding to action, minor, moderate, and major flooding for 3,490 of these stream gauge locations by coordinating with local stakeholders. Thus, there is a subset of the USGS network which has NWS-defined flooding thresholds, which is valuable information for modeling and diagnostics. The definition of action stage is the stage at which NWS forecasters take "mitigation action for possible significant hydrologic activity" and it often corresponds to bankfull conditions. In fact, 41% of the USGS stations have identical action and bankfull stages, differing by only 1.3% on an average.

Gauges that are impacted by regulation or diversion are further screened out using the regulation codes supplied by the USGS. In this database, a flood event is defined as the period when streamflow is above the defined action stage for that gauge. If there is a 24-h period with discharge values below action stage, then the events prior to and following this gap are considered as separate. The database contains the start and

Table 1
Geomorphologic Parameters Included in This Study

Geomorphologic parameter	Details
First moment of flow distance (G1)	Catchment-averaged flow distance (Explained in Equation 2).
Second moment of flow distance (G2)	Explained in Equation 2.
Basin area	Total upstream area that contributes runoff.
Shape factor	A dimensionless number that is given by drainage area divided by square of the main channel length, $K = \left(\text{Drainage Area} / \text{Channel length}^2\right)$.
River length	Measured along a line centered from the basin outlet to the intersection of the extended main channel and the basin boundary.
Relief ratio	Relief is the difference in elevation between the outlet and the highest point in the basin and relief ratio is relief divided by the basin length. It is a measure of the basin-wide river slope. Higher the relief ratio, higher is the runoff and shorter is the flooding rise time.
Slope index	Slope between two points along the main channel upstream from the mouth of the basin at distances equal to 10% and 85% of the total main-channel length (Costa, 1987).
Slope to outlet	Local slope computed at a distance of 1 km over the basin outlet.
Basin curve number	Soil Conservation Service Curve Number (SCS-CN) is an empirical parameter that characterizes the runoff properties for a particular soil and ground cover (United States Soil Conservation Service, 1972).
Kfact	Relative index of susceptibility of bare, cultivated soil to particle detachment and transport by rainfall.
Rock depth	Depth to bedrock at the outlet.
First-order channel frequency	Morisawa (1959)

end time when the flow first exceeded and dropped below the action stage threshold respectively, along with the time and magnitude of peak flow. The maximum basin area in this study is ~45,000 km^2 with a median area of 890 km^2.

A natural flood generally starts because of snowmelt and/or intense rainfall. But, the physiography of the basin and sub-basin scale variability of rainfall will dictate the speed of conveyance of water through the channel network and the magnitude of the peak discharge. Since the goal of this study is to understand the relative impact of rainfall variability and catchment features on flooding, the flood event database is enhanced with attributes representing various landscape properties such as vegetation, topography, climatology, and soil. Several geomorphological parameters were derived from the digital elevation model (DEM) data of the National Elevation Dataset (NED; http://ned.usgs.gov/) as potential explanatory variables of flash flooding. Flow accumulation and flow direction information was extracted by delineating basins with USGS stations. The National Hydrography Dataset (NHD; http://nhd.usgs.gov/) was used to resample (averaging) the 30-m DEM to a 1-km grid to ensure compatibility between DEM-based flow accumulations and the actual river network across the Continental United States (CONUS). The DEM was kept at 1-km in order to match the resolution of the precipitation observation data set. Everything was kept at a consistent resolution for ease of computation and analysis. The geomorphologic parameters for delineated catchments were extracted from these grids using custom libraries. Variables representing soil properties such as mean depth-to-bedrock and K-factor (erodability) were derived from the STATSGO database (Miller & White, 1998) while land cover and land use data from the National Land Cover Dataset (Fry et al., 2011) were used to estimate the runoff curve number. Lastly, the hydroclimatic variables of mean annual precipitation and temperature were extracted from the 30-year data sets (for period 1981–2010) prepared by the PRISM Climate Group of Oregon State University (http://www.prism.oregonstate.edu/normals/). The static spatially distributed basin attributes included in this study are summarized in Table 1.

2.2. Multi Radar Multi Sensor (MRMS) Rainfall Reanalysis Data

Traditionally, rainfall data have been collected using manual and automatic rain gauges. The process has now evolved with radars providing rainfall data at fine spatial and temporal scale with near real-time updates over large areas. An increasingly extensive coverage of radars has led to the development of mosaic

radar rainfall products over the CONUS with high spatio-temporal resolution. The MRMS project, initiated by the NOAA NSSL, has significantly advanced the way precipitation is estimated by producing a seamless high-resolution data set that updates every two minutes without human intervention. A complete description of the MRMS system can be found in Zhang et al. (2015) along with the Quantitative Precipitation Estimation (QPE) generation process that comes from the preceding National Mosaic and Multi-Sensor QPE (NMQ) system (Zhang et al., 2011). The MRMS system currently centralizes collection and collation of data from 180 operational radars and ~7,000 h gauges across the CONUS and southern Canada. The radar data are integrated with atmospheric environmental data, satellite data, and lightning and rain gauge observations to generate a suite of products suitable for weather and hydrologic modeling (Zhang et al., 2015). Recent advances in MRMS precipitation estimation using multi-sensor approaches and attenuation-based estimators in rain has yielded improved accuracy (Zhang et al., 2020). The use of a multi-sensor network enhances rainfall estimation accuracy compared to a single-radar framework. It addresses the issue of significant rainfall estimation errors offsetting the improvements in hydrologic modeling accuracy due to incorporation of rainfall spatial variability (Ogden et al., 2000; Quintero et al., 2012; Schröter et al., 2011; Villarini et al., 2010).

The MRMS CONUS domain is bounded by latitudes 20°–50°N and longitudes 130°–60°W. The radar coverage is not uniform across the country as the western CONUS has large areas with high radar beam heights, which decreases the accuracy of surface precipitation estimation (Kirstetter et al., 2013). This information is used for quality control of the data set used in this study. A reanalysis MRMS product has been recently produced for a period from 2001 to 2011 (Zhang & Gourley, 2018). This reanalysis was performed on the raw, publicly available NEXRAD data archive available from Amazon Web Services (https://aws.amazon.com/public-datasets/nexrad/). The reanalysis domain is analogous to the MRMS domain with products at 0.01° pixel grid resolution for a total of 24,500,000 grid cells. The primary differences with the reanalysis data set compared to the operational MRMS QPE products are the 5-min time step and the rainfall rates are estimated from the vertical structure of reflectivity values whereas the operational MRMS QPEs benefit from the recently upgraded dual-polarization variables. The rainfall rates produced for this period are used to characterize the rainfall spatial variability and its impact on the flooding events reported in the Unified Flash Flood Database.

2.3. Flash Flood Severity

According to the NWS, flash floods are natural hazards that are characterized by "a rapid and extreme flow of high water into a normally dry area, or a rapid water level rise in a stream or creek above a predetermined flood level, beginning within 6 h of the causative event (e.g., intense rainfall, dam failure, and ice jam)" (2012). A new variable called "Flashiness" was introduced in Saharia et al. (2017) as a measure of flash flood severity and is defined as the difference between the peak discharge and action stage discharge normalized by the flooding rise time and contributing basin area. The flooding rise time is the time elapsed from when the discharge crosses the action stage to the peak flow. The metric is scaled between 0 and 1 with higher values corresponding to more severe floods (Equation 2 in Saharia et al., 2017). The event-based flashiness characterizes the basin response for individual floods, especially in terms of producing a large-magnitude discharge in a short period of time in response to heavy rainfall. A fine-scale precipitation data set such as MRMS and the large number of geomorphological variables included in this study allows us to explore how rainfall spatial variability affects flashiness.

The database was subjected to extensive post-processing based on radar beam height and snow percent of total precipitation in a basin to reduce input uncertainties in modeling results. First, all events that fall in basins with a mean radar beam height of greater than 2 km above the ground level were discarded. This was to ensure that, we only include events for which, we have high-quality radar rainfall data from MRMS. Similarly, all events for basins that get less than 20% of their annual precipitation from snowpack were included. For basins that get greater than 20% of its annual precipitation from snowpack, only events in summer months (May–October) were included.

Finally, a data set of 21,143 flooding events enhanced with corresponding geomorphologic and climatologic variables was compiled for the study. These events happened in 1113 basins located in a variety of climatological and physiological conditions. The location of the outlets of these 1113 basins are overlain on a

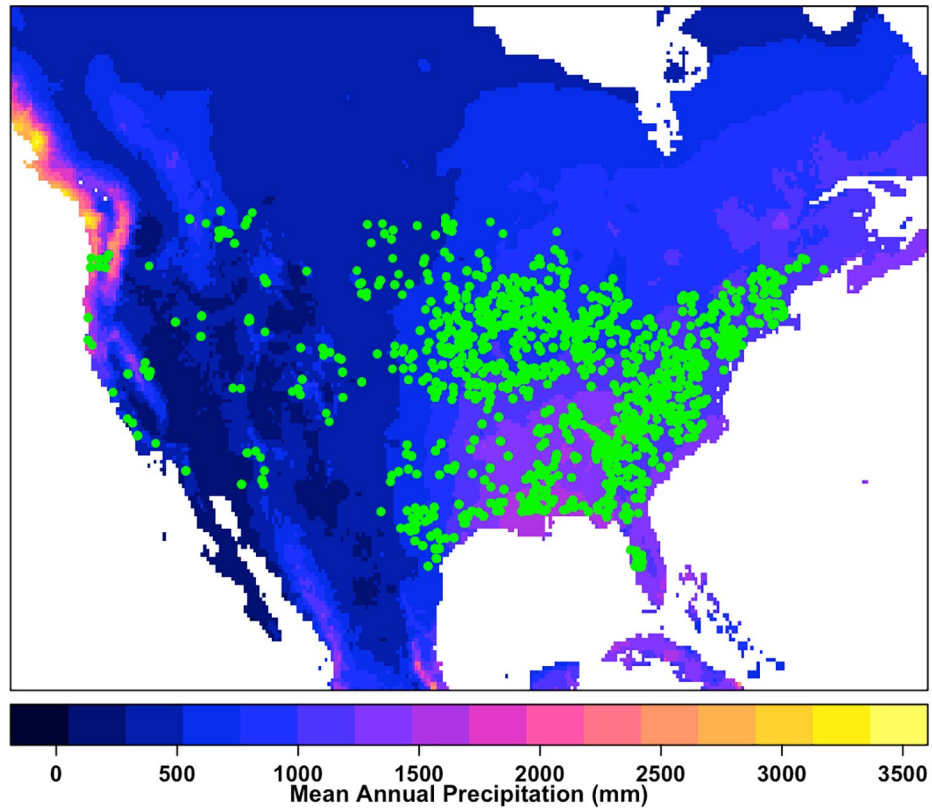

Figure 1. Location of outlets of 1113 US Geological Survey basins across the Continental United States overlain on a map of Mean Annual Precipitation from precipitation-elevation regressions on independent slopes model.

mean annual precipitation map from the precipitation-elevation regressions on independent slopes model (PRISM) (Daly et al., 1994) to show the diversity in settings. The flashiness metric was computed for all 21,143 flooding events Figure 1.

3. Spatial Variability Indices

Indices reflecting the spatial variability of rainfall have been computed for each flooding event in this study. These metrics provide a measure for space-time precipitation organization as a function of the flow distance, that is, distance measured from any point in the basin to the basin outlet along the flow path. To perform event-level characterization, we need metrics that can describe the interaction of precipitation with the basin in a way that can differentiate flooding events from each other. To do this, we introduce the concept of a rain-activated basin, which is the fraction of the basin that experiences a rain event.

The indices are computed on the rainfall accumulated before the peak of the hydrograph (Tq), that is, (Tq–X*Tr), with Tr being the catchment lag time and X denoting the multiplier for the accumulation period. In this study, the catchment lag time is computed as the time interval between the centroid of effective rainfall and peak of the hydrograph. A value of $X = 1.5$ has been adopted in this study as it was found to be the most suitable by Emmanuel et al. (2015) after a duration sensitivity analysis on a simulated database. Moreover, they found similar spatial variability indices to be not very sensitive to the accumulation period and very similar results were obtained for a wide interval period.

We calculated the mean, standard deviation, relative standard deviation, skewness, and kurtosis for the accumulated precipitation, flow distance, and the product of accumulated precipitation and flow distance conditioned on the activated basin. The nth moment of catchment rainfall (p), flow distance, and the product of catchment rainfall and flow distance (c) is defined as:

$$p_n = \frac{1}{A}\int_A \left(p(x,y) - c_p\right)^n dA, \tag{1}$$

$$g_n = \frac{1}{A}\int_A \left(d(x,y) - c_g\right)^n dA, \tag{2}$$

$$\mathrm{pro}_n = \frac{1}{A}\int_A \left(p(x,y)d(x,y) - c_{\mathrm{pro}}\right)^n dA, \tag{3}$$

Where $p(x, y)$ (LT^{-1}) is the accumulated rainfall field at any position (x, y) inside the watershed at a distance $d(x, y)$ (L) from the outlet measured along the flow line and A is the total rain-activated area of the basin. The constants c_p, c_g, and c_{pro} are zero for n equal to unity and they are the mean for the second and higher (central) moments. Note that the first moment of catchment rainfall p_1 is the average rainfall over the basin. Non-dimensional (scaled) spatial moments of catchments rainfall were obtained by taking the ratio between the spatial moments of catchment rainfall and the moments of flow distance, details of which are available in Zoccatelli et al. (2011) and the first two orders are given by the following equations:

$$\Delta_1 = \frac{p_1}{p_0 g_1}, \tag{4}$$

$$\Delta_2 = \frac{1}{g_2 - g_1^2}\left[\frac{p_2}{p_0} - \left(\frac{p_1}{p_0}\right)^2\right]. \tag{5}$$

The first scale moment (Δ_1) describes the location of the catchment rainfall centroid with respect to the catchment centroid. A value of Δ_1 close to 1 represents either a spatially uniform rainfall distribution or rainfall concentrated close to the catchment centroid; while a value less than one describes a rainfall distributed near the basin outlet, and values greater than one represent a rainfall distributed toward the headwaters. The second scaled moment (Δ_2) represents the dispersion of the rainfall-weighted flow distances about their mean value with respect to the dispersion of the flow distances. A value of Δ_2 close to 1 reflects a near-uniform rainfall distribution in the basin, while a value less than 1 indicate a unimodal distribution of rainfall along the flow distance.

Further, two more indices proposed by Emmanuel et al. (2015) based on the width function (Kirkby, 1976; Rigon et al., 2016) denoted w, and on the rainfall-weighted width function, denoted w_p, were also computed for all flooding events. The rainfall-weighted width function is defined as:

$$c_p(d) = \frac{\overline{p(d)}}{p_1} c(d), \tag{6}$$

Where d is the distance to the outlet along the flow line, $\overline{p(d)}$ is the rainfall averaged over all pixels at distance d, and p_1 the average rainfall over the basin. Here, w and w_p can be regarded as probability density functions whose cumulative distributions functions are denoted by W and W_p, respectively. The first index, Vertical Gap (VG), is defined as the absolute value of the maximum vertical difference between W and W_p. This criterion is calculated by the Kolmogorov-Smirnov test, which compares two cumulative distributions. VG values close to zero indicate a rainfall distribution with low spatial variability, while higher values of VG indicate greater concentration of the rainfall over a small part of the catchment. The value of VG is obtained for a quantile value $W_p(d_{p,\mathrm{VG}})$ and a flow distance $d_{p,\mathrm{VG}}$ of W_p. The distance d_{VG} associated with the same quantile value is different for W. The second index, Horizontal Gap (HG), is defined as the absolute difference of these two distances normalized by the maximum flow distance. It can be understood as a measure of the deviation between the rainfall weighted flow distances and the flow distances, expressed in distance units. It represents a spatially homogeneous rainfall or concentrated close to the catchment centroid position for values close to zero, while values lower (or greater) than 0 indicate a rainfall distribution downstream (or upstream).

$$\mathrm{VG} = \max_{0 \le d \le d\,\max} \left|W_p(d) - W(d)\right|, \tag{7}$$

$$\mathrm{HG} = \frac{\left|d_{\mathrm{VG}} - d_{p,\mathrm{VG}}\right|}{d_{\max}}. \tag{8}$$

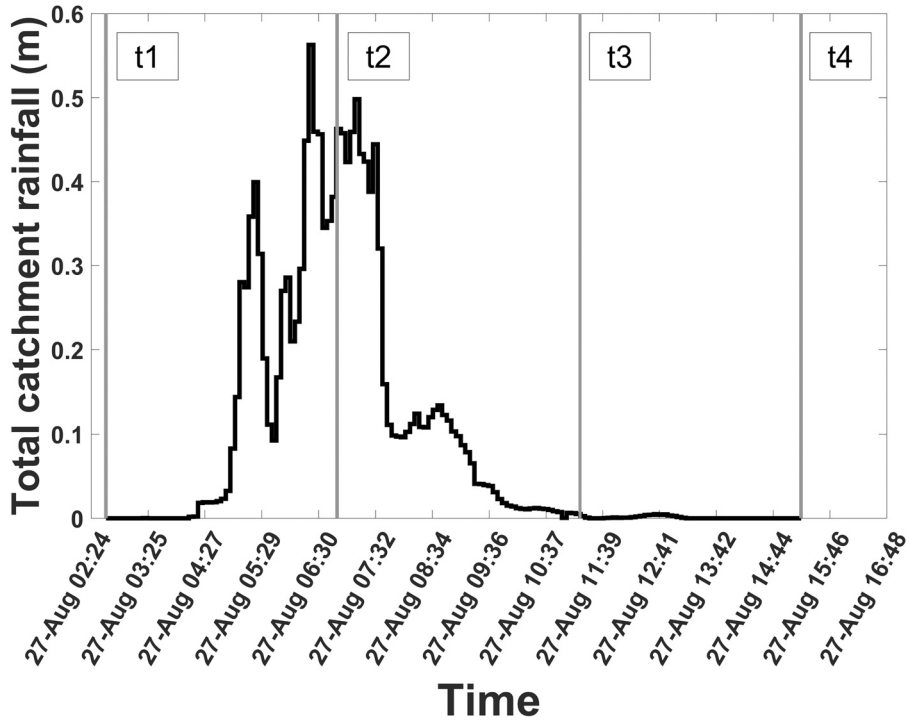

Figure 2. Illustration of rainfall and corresponding flooding for an event on 14–15 March 2003, in the Blue river near McClain in Mississippi with a US Geological Survey gauge of ID 0247500.

The four moments of precipitation, flow distance, and the product of precipitation and flow distance are computed for each of the 21,143 flooding events in the Unified Flash Flood Database between 2002 and 2011.

4. Case Study

A flooding event occurring on August 27, 2006 in the Blue river at Blue Ridge Blvd in Missouri (USGS ID: 6893150) is presented to illustrate the conceptualization of various spatial moments. Important flooding information such as start of the rainfall event (t1), centroid of the rainfall event (t2), start of the flooding event (t3, when streamflow exceeds action stage), and peak discharge (t4), along with associated total catchment rainfall is shown in Figure 2. The corresponding lag time (from centroid of rainfall event to peak discharge) is 8.5 h, while the start of the event was approximately 12 h before the flow reached peak discharge.

Figure 3 shows the flow distance grid, rainfall accumulation grid, and the computation of rainfall moments and width functions. A few of the spatial moments are indicated in the figure. The first (Δ_1) and second order (Δ_2) scaled spatial moments of catchment rainfall for this flooding event are 1.06 and 0.80 respectively. Δ_1 values greater than 1 signify distribution of rainfall toward the headwaters as is confirmed by the rainfall accumulation map of Figure 3b. A value of Δ_2 less than 1 represents a rainfall distribution characterized by a unimodal distribution along the flow distance. This is further confirmed by Figure 3c, where the higher rainfall accumulations are concentrated at longer flow distances (i.e., furthest from catchment outlet). Similarly, horizontal gap (HG) value of 0.06 (greater than zero) indicates rainfall is mainly concentrated in the basin headwaters. While VG of 0.08 (greater than unity) represents concentration of rainfall over a small part of the catchment. One-hundred percent of the basin was activated during the event, based on the number of pixels in the basin that experienced any rain.

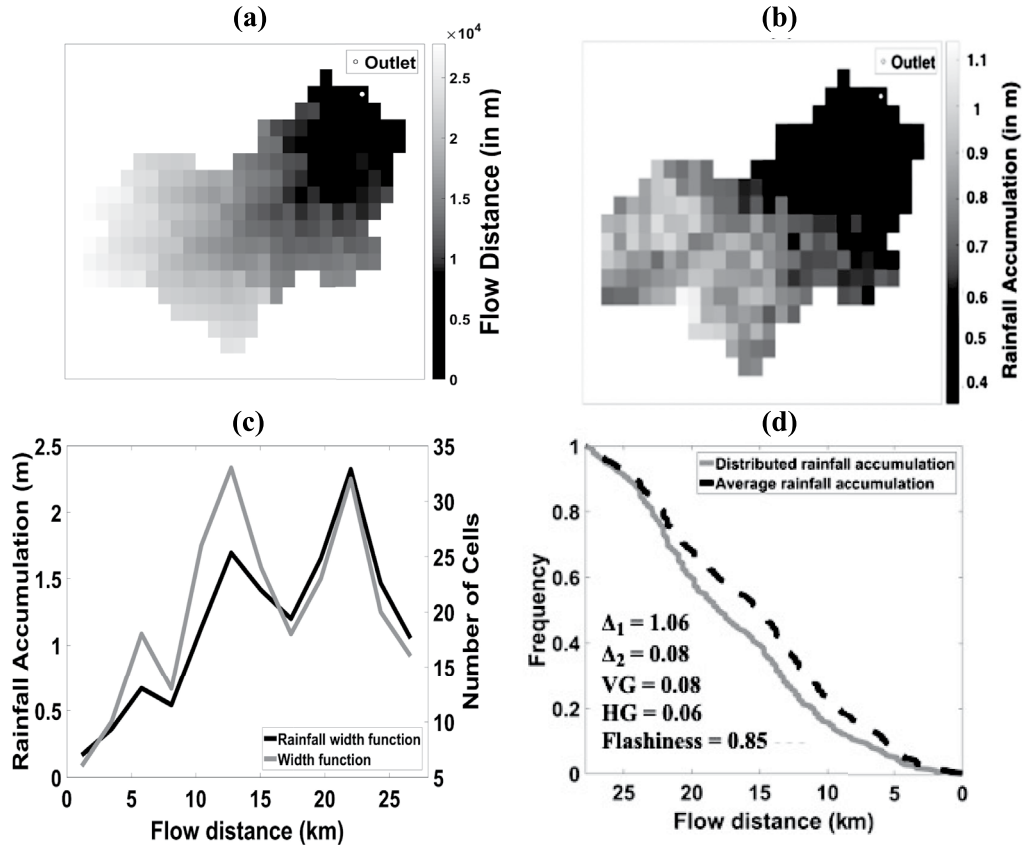

Figure 3. Rainfall spatial variability indices described in Zoccatelli et al. (2011) and Emmanuel et al. (2015) for a flooding event in the Blue river at Blue Ridge Blvd Ext in Missouri with US Geological Survey ID of 6893150 and a catchment area of 241 km^2. The peak flow of the event happened on August 27, 2006 15:15. Here, (a) The flow distances of the basin, (b) Rainfall accumulation field (c) Width function and rainfall width function, (d) Distributions of average and distributed rainfall accumulation along with associated values of Δ_1, Δ_2, horizontal gap, vertical gap, and flashiness.

5. Association of Flashiness With Rainfall and Basin Properties

In order to extract first-order trends, the moments were systematically computed over the entire data set of 21,143 flooding events. Quantile plots were used to analyze the influence of selected event precipitation, climatological, and geomorphological properties on flashiness. Quantile plots display the heterogeneity in the relationships through the conditional distribution of the target variable, with quantiles (1st, 10th, 25th, 50th, 75th, 90th, and 99th). The conditional median describes the first order dependency, while the inter-quartile area estimates the variability in the relationship, and 10th and 90th quantiles describe the conditional extreme values of flashiness.

5.1. Rainfall Variability

Figure 4 shows the quantile plots of flashiness as a function of rainfall-related indices that are among the most important. As shown on Figure 4a, flashiness increases with the mean accumulated precipitation, as expected. Similarly, Figure 4b shows a positive relation between different quantiles of flashiness and the relative standard deviation of accumulated precipitation. Higher values of this index indicate a broader range of rainfall rates, among which high rates are expected to contribute to severe flood processes, while with lower rainfall accumulations competing factors such as antecedent conditions may play a larger role in determining the flood severity. As a result, the median flashiness reaches lower values (0.7) at high relative standard deviation of accumulated precipitation than with events primarily characterized by high accumulated precipitation (0.75). Flashiness shows a decreasing trend with the standard deviation of flow distance (Figure 4c). A low flow distance standard deviation implies that the distance of flow channels from

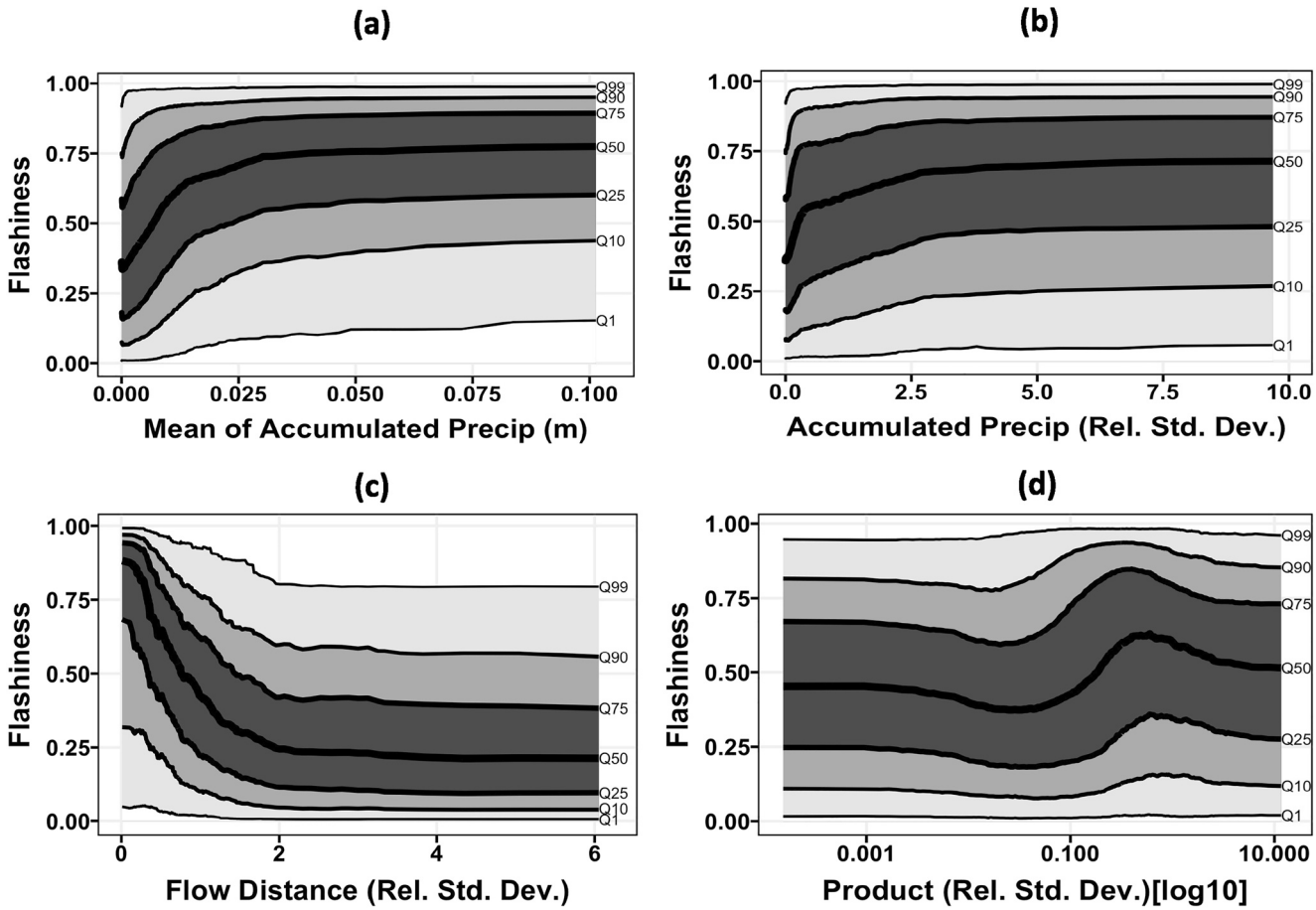

Figure 4. 1st–99th quantile of flashiness versus (a) Mean of accumulated precipitation during the event, (b) Relative standard deviation of accumulated precipitation, (c) Relative standard deviation of flow distance, and (d) Relative standard deviation of the product of accumulated precipitation and flow distance.

the outlet is concentrated around a single value. Water can be conveyed to the outlet at similar times which results in increased flashiness. Higher dispersion of flow distance flattens the hydrograph and generates lower flashiness. Finally, Figure 4d shows the relationship between flashiness and the relative standard deviation of the flow distance weighted by precipitation. However, the quantile plot does not portray a straightforward relationship between the variables, which may be due to the complex interplay of precipitation and topography.

Recall that these quantile plots provide a limited two-dimensional description of the relation between descriptors of precipitation variability and flashiness, while the severity of a flood is concomitantly impacted by many factors driven by the basin physiography and climatology. Thus, a multidimensional modeling approach is required to disaggregate these competing dependencies.

5.2. Basin Properties

The influence of selected physiographic and climatologic variables on flashiness is also analyzed using quantile plots in Figure 5. Steeper basins are expected to experience flashier floods since water travels faster to the outlet through channels. Figure 5a shows the relationship between the flashiness and slope index which describes the main features of the basin slope. Higher slope index (steeper topography) is consistently associated with higher flashiness. Figure 5b shows the relationship between flashiness and the frequency of first-order channels. Basins with more first-order channels increase their conveyance of runoff. There is indeed a slightly positive trend of flashiness with the first-order channel frequency. Figure 5c shows a

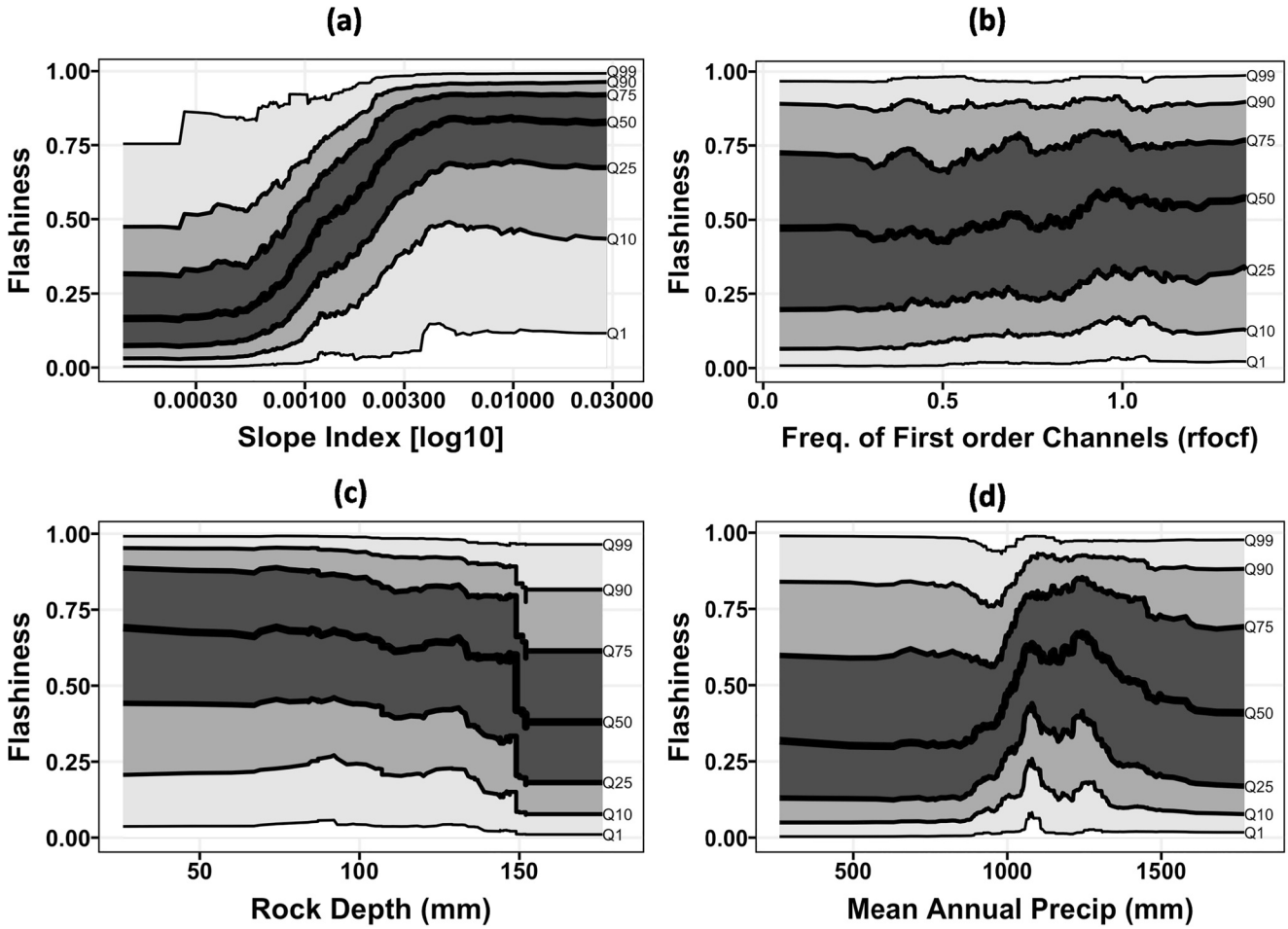

Figure 5. 1st–99th quantile of flashiness versus (a) Slope index, (b) First-order channel frequency, (c) Rock depth, and (d) Mean annual precipitation.

decreasing relationship between flashiness and rock depth (also known as depth to bedrock). For the same prevailing antecedent soil and rainfall conditions, shallower rock depths have lower capacity to absorb and store water and lead to lower interflow, higher runoff, and higher flashiness. A deeper rock depth leads to slower saturation of the soil and less runoff, thus leading to lower flashiness. This decreasing trend is clearly visible in the quantile plot (Figure 5c). Finally, the mean annual precipitation dictates climatological amount of atmospheric water available as input to the basin. Figure 5d shows a nonregular relationship with flashiness, that reflects the complexity of land-atmosphere interactions and storm types that translate rainfall into runoff.

Quantile plots provide valuable insights into the influence of moments of precipitation and flow distances, spatial variability indices, geomorphologic and climatologic variables on flashiness. Yet flooding is a result of complex interactions between many factors and this two-dimensional visual approach is limited to explain competing behaviors. Thus, a multi-dimensional approach is used in the next section to account for the collective influence of many explanatory variables on flashiness. This helps in uncovering the relative impact of different factors on flood events, thus, dramatically improving our ability to diagnose causative processes behind flash floods.

Table 2
Statistical Significance of Explanatory Variables in GAMLSS Model

Type of variable	Variable	*p*-value
Geomorphology	Slope index	$<2 \times 10^{-16}$
Geomorphology	Curve number	$<2 \times 10^{-16}$
Geomorphology	Frequency of first-order channels	$<2 \times 10^{-16}$
Geomorphology	Slope to outlet	$<2 \times 10^{-16}$
Geomorphology	K factor	$<2 \times 10^{-16}$
Geomorphology	Rock depth	$<2 \times 10^{-16}$
Rainfall spatial variability	Flow distance (Mean)	$<2 \times 10^{-16}$
Rainfall spatial variability	Accumulated precipitation (Mean)	$<2 \times 10^{-16}$
Rainfall spatial variability	Δ_1	$<2 \times 10^{-16}$
Rainfall spatial variability	Product (Relative standard deviation)	$<2 \times 10^{-16}$
Climatology	Mean annual temperature	$<2 \times 10^{-16}$
Climatology	Mean temperature of wettest quarter	$<2 \times 10^{-16}$
Climatology	Annual precipitation	$<2 \times 10^{-16}$

Note. Significance is expressed as *p*-value.

6. Multi-Dimensional Modeling of Flash Flood Severity

6.1. The Model

In this work, the complex relationship between the explanatory variables and flashiness is analyzed through conditional distribution functions using the generalized additive models for location, scale, and shape (Rigby & Stasinopoulos, 2005) technique. GAMLSS was proposed to overcome some of the limitations associated with the widely used generalized additive models (Hastie & Tibshirani, 1990), generalized linear models (McCullagh et al., 1989), and generalized additive mixed models (Fahrmeir & Lang, 2001). GAMLSS is an extension over the traditional frameworks and offers higher flexibility as the response variable, which can be continuous, discrete, or mixed, can follow a general distribution function instead of being restricted to the exponential family. The underlying assumption of GAMLSS models is that the response variable (flashiness) is a random variable that follows a known parametric distribution with density f conditioned on different values of the explanatory variables listed in Table 2. The distribution parameters are related to explanatory variables using linear/nonlinear or smooth link functions such as splines. Due to its flexibility, GAMLSS has been used to model various hydrometeorological variables such as precipitation rates (Kirstetter et al., 2015), parameters of the kinematic wave routing parameters (Vergara et al., 2016), and flash flood severity (Saharia et al., 2017). More detailed descriptions of GAMLSS are available, particularly on model fitting and selection (Akantziliotou et al., 2002; Rigby & Stasinopoulos, 2005; Stasinopoulos & Rigby, 2007). Fitting a model involves several steps that include identifying a distribution suitable for describing the response variable, possible explanatory variables, and the link functions. Optimal model selection is based on the maximum likelihood principle and fitting improvement in terms of statistics such as the Akaike Information Criterion (AIC), the Schwarz Bayesian Criterion (SBC) and the generalized AIC (Stasinopoulos & Rigby, 2007). Details on how to select meaningful explanatory variables through forward, backward, and stepwise procedures, as well as diagnostic plots to avoid overfitting are available in Stasinopoulos and Rigby (2007). The GAMLSS modeling has been performed using the gamlss package available for the R language.

Several distributions were tested (e.g., normal, lognormal, and Gumbel) and their goodness-of-fit was checked following Stasinopoulos and Rigby (2007). The beta distribution was identified as the most appropriate distribution for modeling the dependence of flashiness on various geomorphological, climatological, and rainfall variables by using the AIC and by checking the normality and independence of residuals. The original beta distribution is given by:

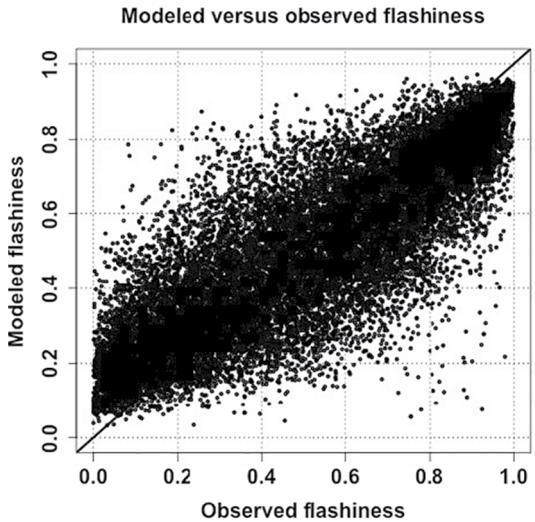

Figure 6. Scatter plot of modeled versus observed flashiness. Correlation = 0.83.

$$f\left(y|\alpha,\beta\right) = \frac{1}{B\left(\alpha,\beta\right)} y^{\alpha-1}\left(1-y\right)^{\beta-1}, \tag{9}$$

for $y = (0, 1)$, $\alpha > 0$ and $\beta > 0$. In the GAMLSS implementation, $\alpha = \mu$ and $\beta > \sigma$ where μ (representing location) and σ (representing scale) are the distribution parameters. The function given in Equation 5 was used to model the conditional flashiness distributions, where the location μ is linked to the expected flashiness value, and the scale σ gives the uncertainty around the expected flashiness. The model is further refined through an iterative procedure of trying various combinations of explanatory variables by using domain knowledge of individual variables and diagnostics. To relate explanatory variables and the beta distribution parameters, penalized splines are used as link functions for fitting trends for each parameter as they offer more flexibility in modeling complex nonlinear relationships. The variables that were retained in the final model are presented in Table 2 along with their corresponding statistical significance p-values. A small p-value indicates there is an association between the explanatory variables and flashiness.

Figure 6 shows a scatter plot of the systematic part (i.e., parameter μ of the beta distribution) of modeled versus observed flashiness with a correlation of 0.83. Thus, the model exhibits significant explanatory power in modeling event flashiness, thereby increasing our confidence in the results to explain the relative impact of various parameters.

6.2. Conditional Estimates of Explanatory Variables

GAMLSS is an additive model and allows us to analyze the influence of individual predictors on the response variable (i.e., flashiness). A partial term plot is a powerful diagnostic tool for disaggregating competing influences. It shows the marginal effect one predictor has on the predicted outcome by averaging all other predictors and plotting the response as a function of the predictor of interest. Figures 7 and 8 show the partial prediction of the flashiness based on a few of the event rainfall, climatological, and geomorphological variables included in the final model.

Figure 7a illustrates how the mean of the accumulated precipitation causes an inflection in flashiness as it increases. This indicates that the physiography of the basin dampens the effect of rainfall at lower values, but rainfall overwhelms other factors resulting in a higher contribution to flashiness at upper ranges. This effect is muted in the equivalent quantile plot that explores first-order dependency in this relationship. The partial plot of Figure 7b shows how increasing occurrence of high rainfall values (i.e., high relative standard deviation of the accumulated precipitation) relates to more severe floods. Figure 7c confirms the dampening effect of dispersed precipitation with respect to the flow paths with an increase of relative standard deviation of flow distance. Similarly, Figure 7d shows a clearly monotonously decreasing relationship between flashiness and the relative standard deviation of the rainfall weighted flow distance. One can note that this relationship appears more clearly than through the unidimensional approach of quantile plots as shown in Figure 4d.

The contribution of geomorphological and climatological variables is similarly exhibited in Figure 8. In Figure 8a, greater slope of a basin lowers travel time for runoff, and hence an increasing trend with flashiness as observed. Similarly, Figure 8b shows a clearly increasing trend of first-order channel frequency with flashiness. While this relationship is expected as larger number of channels means greater water carrying capacity, the dependency was not entirely clear from the quantile plot. Figure 8c shows how the increase in rock depth, that is, the capacity for infiltration and storage of water, decreases flashiness. Finally, the mean annual precipitation shows a clearly increasing trend with flashiness. Higher availability of atmospheric water in the form of rainfall is expected to lead to higher flashiness, though this relationship was difficult to ascertain from the quantile plots.

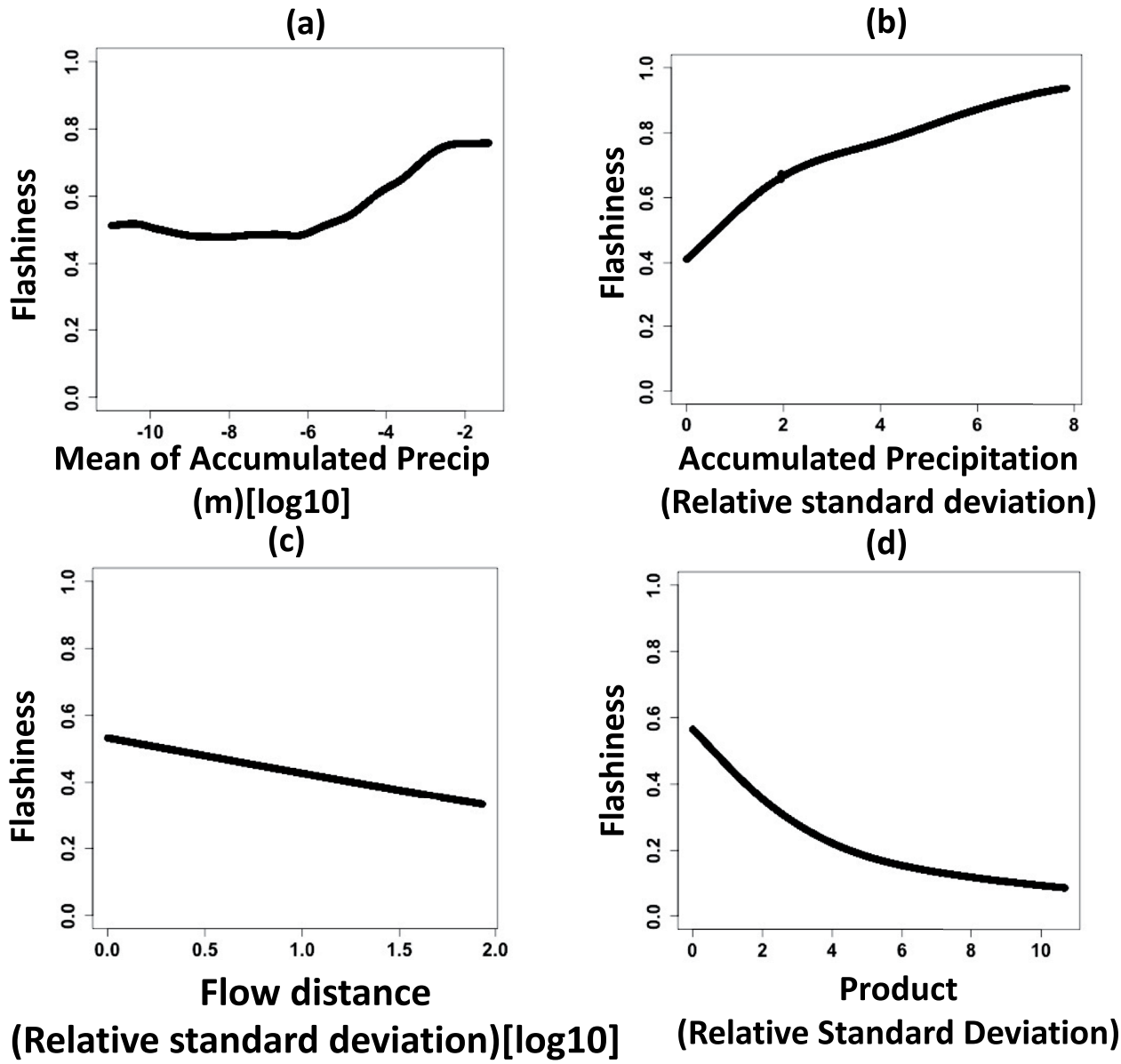

Figure 7. Relative contribution on flashiness by rainfall parameters such as: (a) Mean of accumulated precipitation during the event, (b) Relative standard deviation of accumulated precipitation, (c) Relative standard deviation of flow distance, and (d) Relative standard deviation of the product of accumulated precipitation and flow distance.

This clearly underscores the importance of accounting for rainfall spatial variability in modeling and, in so far as the authors are aware, is the first quantification of this dependence varying with scale.

7. Conclusions

The goal of this study is to quantify the impact of rainfall spatial variability on flash flood severity at the event-scale using a large data set of observations. Flash flood severity, or flashiness, as defined in Saharia et al. (2017), represents the potential of a basin to produce severe floods by encompassing both the timing and magnitude aspects of a flood. A robust methodology including many rainfall spatial variability indices, climatological, and geomorphological variables was used to analyze 21,143 flooding events and improve upon the existing body of knowledge primarily based on case studies and simulations. Complex relationships between the flashiness and a large number of explanatory variables such as the moments of

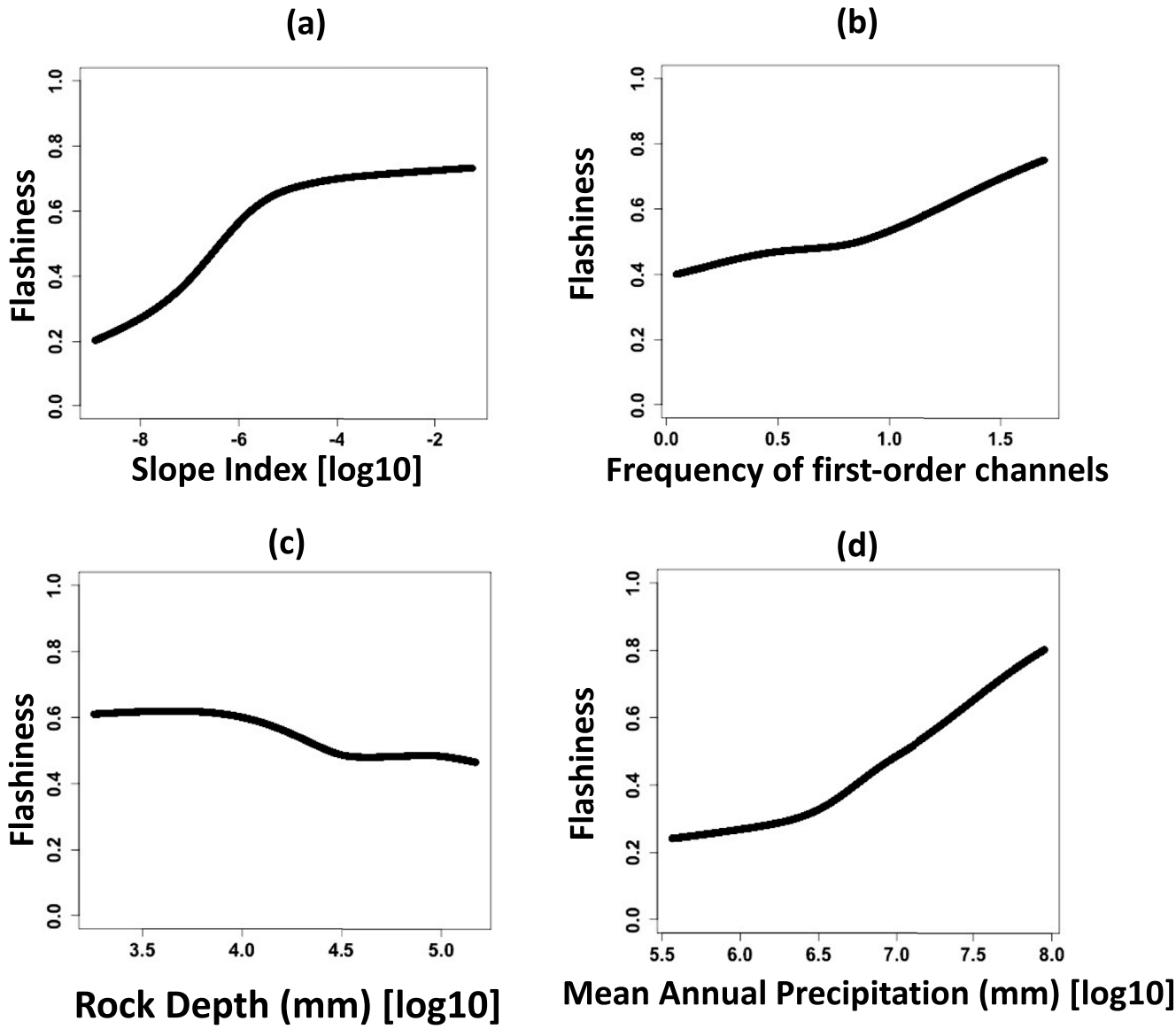

Figure 8. Relative contribution on flashiness by different geomorphologic parameters: (a) Slope index, (b) First-order channel frequency, (c) Rock depth, and (d) Mean annual precipitation.

rainfall and flow distance, spatial variability indices, climatological, and geomorphologic factors were modeled using the GAMLSS multidimensional framework. Along with the variability of these relationships, the relative influences of these factors on flashiness were also assessed, thereby, yielding an improved understanding of these dependencies. The findings are summarized below:

1. A large number of variables were used to model event flashiness. Geomorphologic variables such as slope index, curve number, slope to outlet etc., were found to be important. Variables describing the spatial organization of rainfall such as the first scaled moment, relative standard deviation of the product of rainfall accumulation and flow distance were also found to be significant.
2. The systematic part (i.e., parameter μ of the beta distribution) of the multidimensional model yielded a correlation of 0.83 between modeled and observed flashiness, which means there is adequate skill in the model to explain these dependencies.
3. The contribution of rainfall spatial variability on flashiness was found on par with geomorphology and climatology. There is an inflection point in the relationship between the mean of the accumulated precipitation and flashiness. This is due to the physiography of the basin dampening the effect of lower

rainfall values, while higher rainfall overwhelms other factors and primarily contributes to flashiness. Quantile plots display a nonregular relationship between mean annual precipitation and flashiness, which reflects the complexity of land-atmosphere interactions and storm types that translate rainfall into runoff. The partial term plots reveal that increased flashiness is associated with higher basin slope, higher first-order channel frequency, and higher occurrence of high rainfall values (i.e., high relative standard deviation of the accumulated precipitation). The increasing occurrence of high rainfall values (i.e., high mean and relative standard deviation of accumulated precipitation) leads to more severe floods. However, increasing dispersion in precipitation with respect to the flow path has a dampening effect on floods severity, as flashiness decreases with the relative standard deviation of rainfall weighted flow distance. These findings, based on unprecedented spatial and temporal representativeness, highlight the importance of accounting for rainfall spatial variability in hydrologic modeling.

This study provides the first multi-scale quantification of the relative impact of rainfall spatial variability, climatology, and basin physiography on the flash flooding response. Results can contribute to improving the spatial flash flood guidance approach proposed by Douinot et al. (2016), which only uses the first and second scaled spatial moments proposed by Zoccatelli et al. (2010). Improved understanding of the dependence of hydrologic process on the organization of rainfall and the geomorphology at catchment scale will be useful in improving physics-based hydrological models. In the future, we will derive threshold values of these variability indices, that will identify basins most amenable to distributed hydrologic modeling where significant rainfall spatial variability drives the variability in basin response. The analysis framework will complement our understanding of hydrologic processes and their representation in modeling.

Conflict of Interest

The authors declare no conflicts of interest relevant to this study.

Data Availability Statement

The data sets employed in this research can be found in the following repositories: MRMS reanalysis (http://edc.occ-data.org/nexrad/mosaic/); Unified Flash Flood Database (https://blog.nssl.noaa.gov/flash/database/); PRISM (https://prism.oregonstate.edu/); National Elevation Dataset (http://ned.usgs.gov/); and the National Hydrography Dataset (https://nhd.usgs.gov/).

Acknowledgments
This work was supported by the Disaster Relief Appropriations Act of 2013 (P.L. 113-2), which funded NOAA research grant NA14OAR4830100. P. Kirstetter acknowledges support through the NASA Precipitation Measurement Missions award 80NSSC19K0681, the NASA Ground Validation Program award NNX16AL23G, the NOAA GOES-R Risk Reduction Science Program award NA16OAR4320115, and the NOAA award NA16OAR4320115.

References

Adams, R., Western, A. W., & Seed, A. W. (2012). An analysis of the impact of spatial variability in rainfall on runoff and sediment predictions from a distributed model. *Hydrological Processes*, *26*(21), 3263–3280. https://doi.org/10.1002/hyp.8435

Akantziliotou, K., Rigby, R., & Stasinopoulos, D. (2002). The R implementation of generalized additive models for location, scale and shape. In *Statistical modelling in society: Proceedings of the 17th International Workshop on Statistical Modelling* (pp. 75–83). Statistical Modelling Society.

Anquetin, S., Braud, I., Vannier, O., Viallet, P., Boudevillain, B., Creutin, J.-D., & Manus, C. (2010). Sensitivity of the hydrological response to the variability of rainfall fields and soils for the Gard 2002 flash-flood event. *Journal of Hydrology*, *394*(1–2), 134–147. https://doi.org/10.1016/j.jhydrol.2010.07.002

Brath, A., Montanari, A., & Toth, E. (2004). Analysis of the effects of different scenarios of historical data availability on the calibration of a spatially-distributed hydrological model. *Journal of Hydrology*, *291*(3), 232–253. https://doi.org/10.1016/j.jhydrol.2003.12.044

Cole, S. J., & Moore, R. J. (2008). Hydrological modelling using raingauge- and radar-based estimators of areal rainfall. *Journal of Hydrology*, *358*(3–4), 159–181. https://doi.org/10.1016/j.jhydrol.2008.05.025

Costa, J. E. (1987). Hydraulics and basin morphometry of the largest flash floods in the conterminous United States. *Journal of Hydrology*, *93*(3–4), 313–338. https://doi.org/10.1016/0022-1694(87)90102-8

Daly, C., Neilson, R. P., & Phillips, D. L. (1994). A statistical-topographic model for mapping climatological precipitation over mountainous terrain. *Journal of Applied Meteorology*, *33*(2), 140–158. https://doi.org/10.1175/1520-0450(1994)033<0140:ASTMFM>2.0.CO;2

Douinot, A., Roux, H., Garambois, P.-A., Larnier, K., Labat, D., & Dartus, D. (2016). Accounting for rainfall systematic spatial variability in flash flood forecasting. *Journal of Hydrology*, *541*, 359–370. https://doi.org/10.1016/j.jhydrol.2015.08.024

Emmanuel, I., Andrieu, H., Leblois, E., Janey, N., & Payrastre, O. (2015). Influence of rainfall spatial variability on rainfall-runoff modelling: Benefit of a simulation approach? *Journal of Hydrology*, *531*, 337–348. https://doi.org/10.1016/j.jhydrol.2015.04.058

Fabry, F. (1996). On the determination of scale ranges for precipitation fields. *Journal of Geophysical Research*, *101*(D8), 12819–12826. https://doi.org/10.1029/96JD00718

Fahrmeir, L., & Lang, S. (2001). Bayesian semiparametric regression analysis of multicategorical time-space data. *Annals of the Institute of Statistical Mathematics*, *53*(1), 11–30. https://doi.org/10.1023/a:1017904118167

Fry, J. A., Xian, G., Jin, S., Dewitz, J. A., Homer, C. G., Yang, L., et al. (2011). Completion of the 2006 national land cover database for the Conterminous United States. *Photogrammetric Engineering & Remote Sensing*, *77*(9), 858–864.

Gourley, J. J., Erlingis, J. M., Smith, T. M., Ortega, K. L., & Hong, Y. (2010). Remote collection and analysis of witness reports on flash floods. *Journal of Hydrology*, *394*(1), 53–62. https://doi.org/10.1016/j.jhydrol.2010.05.042

Gourley, J. J., Hong, Y., Flamig, Z. L., Arthur, A., Clark, R., Calianno, M., et al. (2013). A unified flash flood database across the United States. *Bulletin of the American Meteorological Society*, *94*(6), 799–805. https://doi.org/10.1175/BAMS-D-12-00198.1

Hastie, T. J., & Tibshirani, R. J. (1990). *Generalized additive models* (Vol. 43). CRC Press.

Kim, B. S., Kim, B. K., & Kim, H. S. (2008). Flood simulation using the gauge-adjusted radar rainfall and physics-based distributed hydrologic model. *Hydrological Processes*, *22*(22), 4400–4414. https://doi.org/10.1002/hyp.7043

Kirkby, M. J. (1976). Tests of the random network model, and its application to basin hydrology. *Earth Surface Processes*, *1*(3), 197–212. https://doi.org/10.1002/esp.3290010302

Kirstetter, P.-E., Andrieu, H., Boudevillain, B., & Delrieu, G. (2013). A Physically based identification of vertical profiles of reflectivity from volume scan radar data. *Journal of Applied Meteorology and Climatology*, *52*(7), 1645–1663. https://doi.org/10.1175/JAMC-D-12-0228.1

Kirstetter, P.-E., Gourley, J. J., Hong, Y., Zhang, J., Moazamigoodarzi, S., Langston, C., & Arthur, A. (2015). Probabilistic precipitation rate estimates with ground-based radar networks. *Water Resources Research*, *51*(3), 1422–1442. https://doi.org/10.1002/2014WR015672

Lobligeois, F., Andréassian, V., Perrin, C., Tabary, P., & Loumagne, C. (2014). When does higher spatial resolution rainfall information improve streamflow simulation? An evaluation using 3620 flood events. *Hydrology and Earth System Sciences*, *18*(2), 575–594. https://doi.org/10.5194/hess-18-575-2014

Looper, J. P., & Vieux, B. E. (2012). An assessment of distributed flash flood forecasting accuracy using radar and rain gauge input for a physics-based distributed hydrologic model. *Journal of Hydrology*, *412*(413), 114–132. https://doi.org/10.1016/j.jhydrol.2011.05.046

Marani, M. (2005). Non-power-law-scale properties of rainfall in space and time. *Water Resources Research*, *41*(8), W08413. https://doi.org/10.1029/2004WR003822

Marra, F., & Morin, E. (2015). Use of radar QPE for the derivation of intensity-duration-frequency curves in a range of climatic regimes. *Journal of Hydrology*, *531*, 427–440. https://doi.org/10.1016/j.jhydrol.2015.08.064

McCullagh, P., Nelder, J. A., & McCullagh, P. (1989). *Generalized linear models* (Vol. 2). Chapman and Hall London.

Mei, Y., Anagnostou, E. N., Stampoulis, D., Nikolopoulos, E. I., Borga, M., & Vegara, H. J. (2014). Rainfall organization control on the flood response of mild-slope basins. *Journal of Hydrology*, *510*, 565–577. https://doi.org/10.1016/j.jhydrol.2013.12.013

Merz, R., & Blöschl, G. (2004). Regionalisation of catchment model parameters. *Journal of Hydrology*, *287*(1–4), 95–123. https://doi.org/10.1016/j.jhydrol.2003.09.028

Miller, D. A., & White, R. A. (1998). A Conterminous United States multilayer soil characteristics dataset for regional climate and hydrology modeling. *Earth Interactions*, *2*(2), 1–26. https://doi.org/10.1175/1087-3562(1998)002<0001:ACUSMS>2.3.CO;2

Morisawa, M. E. (1959). *Relation of quantitative geomorphology to stream flow in representative watersheds of the Appalachian Plateau Province (Technical Report No. No. CU-TR-20)*. Columbia University.

Nicótina, L., Celegon, E. A., Rinaldo, A., & Marani, M. (2008). On the impact of rainfall patterns on the hydrologic response. *Water Resources Research*, *44*(12). https://doi.org/10.1029/2007WR006654

Obled, C., Wendling, J., & Beven, K. (1994). The sensitivity of hydrological models to spatial rainfall patterns: An evaluation using observed data. *Journal of Hydrology*, *159*(1), 305–333. https://doi.org/10.1016/0022-1694(94)90263-1

Ogden, F. L., Sharif, H. O., Senarath, S. U. S., Smith, J. A., Baeck, M. L., & Richardson, J. R. (2000). Hydrologic analysis of the Fort Collins, Colorado, flash flood of 1997. *Journal of Hydrology*, *228*(1–2), 82–100. https://doi.org/10.1016/S0022-1694(00)00146-3

Ortega, K. L., Smith, T. M., Manross, K. L., Kolodziej, A. G., Scharfenberg, K. A., Witt, A., & Gourley, J. J. (2009). The severe hazards analysis and verification experiment. *Bulletin of the American Meteorological Society*, *90*(10), 1519–1530. https://doi.org/10.1175/2009BAMS2815.1

Pokhrel, P., & Gupta, H. V. (2011). On the ability to infer spatial catchment variability using streamflow hydrographs. *Water Resources Research*, *47*(8). https://doi.org/10.1029/2010WR009873

Quintero, F., Sempere-Torres, D., Berenguer, M., & Baltas, E. (2012). A scenario-incorporating analysis of the propagation of uncertainty to flash flood simulations. *Journal of Hydrology*, *460*(461), 90–102. https://doi.org/10.1016/j.jhydrol.2012.06.045

Rigby, R. A., & Stasinopoulos, D. M. (2005). Generalized additive models for location, scale and shape. *Journal of the Royal Statistical Society: Series C (Applied Statistics)*, *54*(3), 507–554. https://doi.org/10.1111/j.1467-9876.2005.00510.x

Rigon, R., Bancheri, M., Formetta, G., & de Lavenne, A. (2016). The geomorphological unit hydrograph from a historical-critical perspective: Geomorphological unit hydrograph. *Earth Surface Processes and Landforms*, *41*(1), 27–37. https://doi.org/10.1002/esp.3855

Rodriguez- Iturbe, I., & Rinaldo, A. (1997). *Fractal river basins: Chance and self-organization*. Cambridge University Press. Retrieved from https://infoscience.epfl.ch/record/141481

Saharia, M., Kirstetter, P.-E., Vergara, H., Gourley, J. J., Hong, Y., & Giroud, M. (2017). Mapping flash flood severity in the United States. *Journal of Hydrometeorology*, *18*(2), 397–411. https://doi.org/10.1175/JHM-D-16-0082.1

Sangati, M., Borga, M., Rabuffetti, D., & Bechini, R. (2009). Influence of rainfall and soil properties spatial aggregation on extreme flash flood response modelling: An evaluation based on the Sesia river basin, North Western Italy. *Advances in Water Resources*, *32*(7), 1090–1106. https://doi.org/10.1016/j.advwatres.2008.12.007

Schröter, K., Llort, X., Velasco-Forero, C., Ostrowski, M., & Sempere-Torres, D. (2011). Implications of radar rainfall estimates uncertainty on distributed hydrological model predictions. *Atmospheric Research*, *100*(2–3), 237–245. https://doi.org/10.1016/j.atmosres.2010.08.014

Sivapalan, M., Takeuchi, K., Franks, S. W., Gupta, V. K., Karambiri, H., Lakshmi, V., et al. (2003). IAHS decade on predictions in ungauged basins (PUB), 2003–2012: Shaping an exciting future for the hydrological sciences. *Hydrological Sciences Journal*, *48*(6), 857–880. https://doi.org/10.1623/hysj.48.6.857.51421

Smith, J. A., Baeck, M. L., Meierdiercks, K. L., Miller, A. J., & Krajewski, W. F. (2007). Radar rainfall estimation for flash flood forecasting in small urban watersheds. *Advances in Water Resources*, *30*(10), 2087–2097. https://doi.org/10.1016/j.advwatres.2006.09.007

Smith, J. A., Baeck, M. L., Meierdiercks, K. L., Nelson, P. A., Miller, A. J., & Holland, E. J. (2005). Field studies of the storm event hydrologic response in an urbanizing watershed. *Water Resources Research*, *41*(10). https://doi.org/10.1029/2004WR003712

Smith, J. A., Baeck, M. L., Morrison, J. E., Sturdevant-Rees, P., Turner-Gillespie, D. F., & Bates, P. D. (2002). The regional hydrology of extreme floods in an urbanizing drainage basin. *Journal of Hydrometeorology*, *3*(3), 267–282. https://doi.org/10.1175/1525-7541(2002)003<0267:TRHOEF>2.0.CO;2

Smith, M. B., Koren, V. I., Zhang, Z., Reed, S. M., Pan, J.-J., & Moreda, F. (2004). Runoff response to spatial variability in precipitation: An analysis of observed data. *Journal of Hydrology*, *298*(1–4), 267–286. https://doi.org/10.1016/j.jhydrol.2004.03.039

Stasinopoulos, D. M., & Rigby, R. A. (2007). Generalized additive models for location scale and shape (GAMLSS) in R. *Journal of Statistical Software*, *23*(7), 1–46. https://doi.org/10.18637/jss.v023.i07

United States Soil Conservation Service. (1972). *SCS national engineering handbook (Supplement A, Section 4, Chapter 10): Hydrology*. Soil Conservation Service, USDA.

Vergara, H., Kirstetter, P.-E., Gourley, J. J., Flamig, Z. L., Hong, Y., Arthur, A., & Kolar, R. (2016). Estimating a-priori kinematic wave model parameters based on regionalization for flash flood forecasting in the Conterminous United States. *Journal of Hydrology*, *541*, 421–433. https://doi.org/10.1016/j.jhydrol.2016.06.011

Vieux, B. E., Park, J.-H., & Kang, B. (2009). Distributed hydrologic prediction: Sensitivity to accuracy of initial soil moisture conditions and radar rainfall input. *Journal of Hydrologic Engineering*, *14*(7), 671–689. https://doi.org/10.1061/(ASCE)HE.1943-5584.0000039

Villarini, G., Krajewski, W. F., Ntelekos, A. A., Georgakakos, K. P., & Smith, J. A. (2010). Towards probabilistic forecasting of flash floods: The combined effects of uncertainty in radar-rainfall and flash flood guidance. *Journal of Hydrology*, *394*(1–2), 275–284. https://doi.org/10.1016/j.jhydrol.2010.02.014

Winchell, M., Gupta, H. V., & Sorooshian, S. (1998). On the simulation of infiltration- and saturation-excess runoff using radar-based rainfall estimates: Effects of algorithm uncertainty and pixel aggregation. *Water Resources Research*, *34*(10), 2655–2670. https://doi.org/10.1029/98WR02009

Woods, R., & Sivapalan, M. (1999). A synthesis of space-time variability in storm response: Rainfall, runoff generation, and routing. *Water Resources Research*, *35*(8), 2469–2485. https://doi.org/10.1029/1999WR900014

Zhang, J., & Gourley, J. (2018). *Multi-radar multi-sensor precipitation reanalysis (version 1.0)*. Open Commons Consortium Environmental Data Commons. https://doi.org/10.25638/EDC.PRECIP.0001

Zhang, J., Howard, K., Langston, C., Kaney, B., Qi, Y., Tang, L., et al. (2015). Multi-radar multi-sensor (MRMS) quantitative precipitation estimation: Initial operating capabilities. *Bulletin of the American Meteorological Society*, *97*(4), 621–638. https://doi.org/10.1175/BAMS-D-14-00174.1

Zhang, J., Howard, K., Langston, C., Vasiloff, S., Kaney, B., Arthur, A., et al. (2011). National mosaic and multi-sensor QPE (NMQ) system: Description, results, and future plans. *Bulletin of the American Meteorological Society*, *92*(10), 1321–1338. https://doi.org/10.1175/2011BAMS-D-11-00047.1

Zhang, J., Tang, L., Cocks, S., Zhang, P., Ryzhkov, A., Howard, K., et al. (2020). A dual-polarization radar synthetic QPE for operations. *Journal of Hydrometeorology*, *21*(11), 2507–2521. https://doi.org/10.1175/JHM-D-19-0194.1

Zoccatelli, D., Borga, M., Viglione, A., Chirico, G. B., & Blöschl, G. (2011). Spatial moments of catchment rainfall: Rainfall spatial organisation, basin morphology, and flood response. *Hydrology and Earth System Sciences*, *15*(12), 3767–3783. https://doi.org/10.5194/hess-15-3767-2011

Zoccatelli, D., Borga, M., Zanon, F., Antonescu, B., & Stancalie, G. (2010). Which rainfall spatial information for flash flood response modelling? A numerical investigation based on data from the Carpathian range, Romania. *Journal of Hydrology*, *394*(1–2), 148–161. https://doi.org/10.1016/j.jhydrol.2010.07.019